analytical chemistry

Letter

Cite This: Anal. Chem. XXXX, XXX, XXX−XXX

pubs.acs.org/ac

Noninvasive and Nondestructive Detection of Cowpea Bruchid within Cowpea Seeds with a Hand-Held Raman Spectrometer

Lee Sanchez,[†,∥] Charles Farber,[†,∥] Jiaxin Lei,[‡] Keyan Zhu-Salzman,[‡] and Dmitry Kurouski*[,†,§]

[†]Department of Biochemistry and Biophysics, Texas A&M University, College Station, Texas 77843, United States

[‡]Department of Entomology, Texas A&M University, College Station, Texas 77843, United States

[§]The Institute for Quantum Science and Engineering, Texas A&M University, College Station, Texas 77843, United States

Supporting Information

ABSTRACT: Insect damage to crops is a serious issue, in particular when the pest dwells within its host. The cowpea bruchid (*Callosobruchus maculatus*) is an herbivore of legumes including beans and peas. The bruchid lays its eggs on the seeds themselves; after hatching, the larvae burrow into and develop inside the seed, complicating detection and treatment. Left unchecked, two insects could destroy up to 50% of 1 ton of harvest cowpea (*Vigna unguiculata*) after several months of storage. In this study, we investigated the possibility of using a hand-held Raman spectrometer to detect the pest during its development within intact cowpeas. Our results show that Raman spectroscopy can detect chemical signatures of bruchid larvae as well as their excrements inside the intact seeds. Additionally, using chemometric methods, we distinguished between healthy and infested seeds as well as among seeds hosting developmentally early or late-stage larvae with high accuracy. This study demonstrates Raman spectroscopy's efficacy in not only detection of pathogens and pests present on the surface of plant leaves and the grain but also inside the seeds. This Raman-based method may prove useful as a rapid means of screening crops for internal pests.

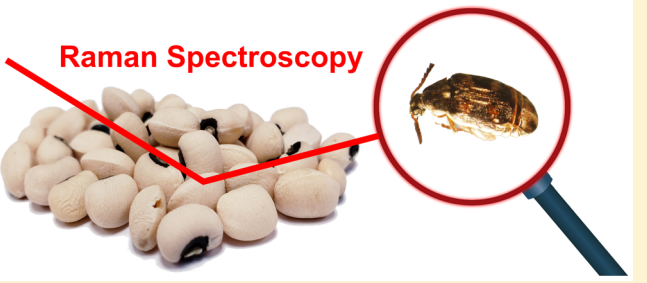

Meeting the dietary needs of the world is a constant issue. Based on recent population growth projections, we will need to produce 70% more food by 2050.[1] There are several strategies to address this challenge: expand agricultural land areas or develop more advanced agriculture. Despite being utilized in many developing countries, the first approach is inefficient, destructive to nature and can offer only a short-term solution for global food security. The second strategy involves advanced plant genetics and plant breeding, as well as development of technologies that would enable timely detection, identification and treatment of plant pathogens and pests.[2]

Raman spectroscopy (RS) is a label-free, noninvasive, nondestructive spectroscopic technique which can be used to determine structure and molecular composition of analyzed specimens. RS efficacy has been shown in food chemistry,[3] electrochemistry,[4] forensics,[5,6] materials science,[7] and many other research areas. For instance, it has been recently demonstrated that RS can be used to monitor changes in protein secondary structure,[8] conduct forensic analysis of body fluids,[5] and detect gunshot residues.[9] Another advantage of RS is its portability, enabling utilization of RS directly in the field.[10]

We have recently demonstrated that a hand-held Raman spectrometer is able to detect and identify fungi-induced diseases on maize.[11] Specifically, we identified whether maize kernels were healthy or infected by *Aspergillus flavus*, *A. niger*, *Fusarium spp.*, or *Diplodia spp.* with high accuracy. This approach is based on pathogen-specific changes to host molecules. We also showed that RS can be used for highly accurate detection and identification of fungal diseases on sorghum and wheat grain. It appeared that RS was capable of diagnosis of simple diseases, such as ergot, that are caused by one pathogen, as well as complex diseases, such as black tip or mold, which were induced by several different pathogens.[12,13] We also showed that RS can be used to determine states of disease development on grain. These results potentially suggest that Raman-based approach for disease detection on plants is sample agnostic.

It is yet to be determined whether RS can be utilized for detection of insect pests hidden inside seeds, fruits and vegetables before visual symptoms develop. In this study, we investigated the possibility of using RS to detect the presence of cowpea bruchid (*Callosobruchus maculatus*) in intact seeds. This insect infests legumes, including cowpea (*Vigna unguiculata*), soybean (*Glycine max*), and mung bean (*Vigna radiata*) not only in the field but also after harvest. Eggs are laid on the seed surface. Hatched larvae burrow into and consume the seeds. The larvae develop through four immature larval stages, before finally pupating and emerging from the

Received: December 1, 2018
Accepted: January 8, 2019
Published: January 8, 2019

DOI: 10.1021/acs.analchem.8b05555
Anal. Chem. XXXX, XXX, XXX−XXX

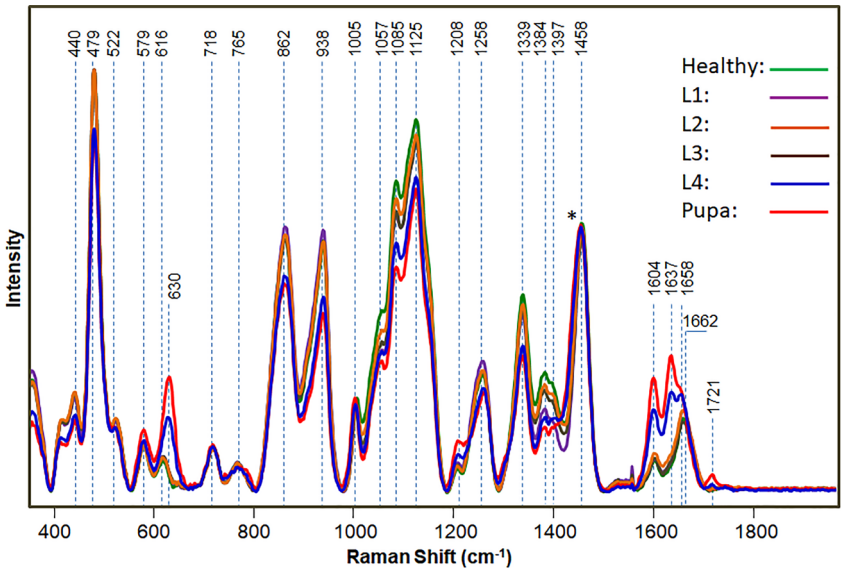

Figure 1. Raman spectra of healthy, uninfested cowpea seeds and seeds infested by bruchids at larval and pupal stages, normalized to the 1458 cm^{-1} peak (indicated by an asterisk (*)). Spectra were acquired with an Agilent Resolve spectrometer with the following parameters: 830 nm excitation, 500 mW power, 1 s acquisition.

seeds as adults. The adults, which do not feed upon the seeds themselves, live for about 10−12 days but are extremely fertile: a single female can lay approximately 100 eggs. This quick life-cycle and high reproduction rate explains their destructiveness: one breeding pair of beetles can destroy half a ton of seeds within half a year.[14]

Using a hand-held Raman spectrometer, we collected spectra from cowpea seeds infested with bruchids at different developmental stages: first, second, third, fourth instar larvae (L1−L4) or pupa (17 seeds per stage, 3 spectra per seed averaged). The respective spectra were averaged and compared to the average Raman spectrum of healthy cowpea seeds (37 seeds, 3 spectra per seed averaged, Figure 1).

Normalizing spectra without an internal standard is challenging. In the acquired spectra, we observed peaks originating from carbohydrates (~55% seed dry weight), proteins (22%), and lignin (5%),[15] each of which exhibit several Raman bands (Table 1, discussed below in detail). Normalization on one particular band out of all observed for the particular class of molecules, such as carbohydrates, may not be appropriate if their intensities change. At the same time, CH_2 vibrations (1458 cm^{-1}) cannot be assigned to any specific class of compounds since this chemical group is present in many organic molecules. Therefore, all reported Raman spectra in the study are normalized on the 1458 cm^{-1} band.

In the Raman spectra collected from L1−L3 seeds, we observed a gradual decrease in the intensities of (C−O−H) vibrational bands (440, 479, 522, 862, 938, 1057, 1085, 1125, 1258, 1339, 1384, 1397 cm^{-1}), whereas drastic changes in these bands were observed in seeds infested by L4 and pupa (Figure 1). These vibrational bands can be assigned to carbohydrates, which include starch and oligo- and monosaccharides. We conducted a series of one-way ANOVA values to evaluate whether observed changes in intensities of select carbohydrate vibrational bands (440, 1057, 1085, and 1125 cm^{-1}) are statistically significant. ANOVAs follwed by Tukey HSD tests revealed that in most cases (1057, 1085, and 1125 cm^{-1}), healthy seeds and seeds hosting L1−L3 were significantly different from those containing L4 or pupa.

Table 1. Vibrational Bands and Their Assignments for Healthy and Bruchid-Infected Cowpea Seeds at L1−L4 and Pupa Stages

band	vibrational mode	assignment
440	skeletal modes of pyranose ring	carbohydrates[3,24]
479	C−C−O and C−C−C deformations; related to glycosidic ring skeletal deformations	carbohydrates[3]
	δ(C−C−C) + τ(C−O) scissoring of C−C−C and out-of-plane bending of C−O	
522	δ(C−C−O) + τ(C−O) of carbohydrates or disulfide bond (S−S) of cysteines	carbohydrates,[3] proteins[25]
579	ν(C−O) + ν(C−C) + δ(C−O−H)	cellulose, lignin[26]
616	δ(C−C−O) of carbohydrates	carbohydrates
630	urate; C−S stretching	urate,[27] cysteine[20]
718	δ(C−C−O) related to glycosidic ring skeletal deformations	carbohydrates[3]
765	δ(C−C−O)	carbohydrates[3]
862	δ(C−C−H) + δ(C−O−C) glycosidic bond; anomeric region	carbohydrates[3]
938	skeletal modes; δ(C−O−C) + δ(C−O−H) + ν(C−O) α-1,4 glycosidic linkages	carbohydrates[28]
1005	phenylalanine ring stretching mode	proteins[17]
1057	ν(C−O) + ν(C−C) + δ(C−O−H)	carbohydrates[3]
1085	ν(C−O) + ν(C−C) + δ(C−O−H)	carbohydrates[3]
1125	ν(C−O) + ν(C−C) + δ(C−O−H)	carbohydrates[3]
1208	aromatic ring modes of phenylalanine and tyrosine	proteins[29]
1258	δ(C−C−H) + δ(O−C−H) + δ(C−O−H)	carbohydrates[3,30]
1339	ν(C−O); δ(C−O−H)	carbohydrates[3]
1384	δ(C−O−H), coupling of the CCH and COH deformation modes	carbohydrates[3]
1397	δ(C−C−H)	carbohydrates[3]
1458	δ(CH) + δ(CH_2) + δ(C−O−H) CH, CH_2, and COH deformations.	aliphatic[3]
1604	ν(C−C) aromatic ring + σ(CH) of carbohydrates, phenylalanine	lignin,[31,32] proteins,[29] ergosterol[33]
1637−1662	C═O stretching, amide I	proteins[25]
1721	C═O stretching	esters[21−23]

DOI: 10.1021/acs.analchem.8b05555
Anal. Chem. XXXX, XXX, XXX−XXX

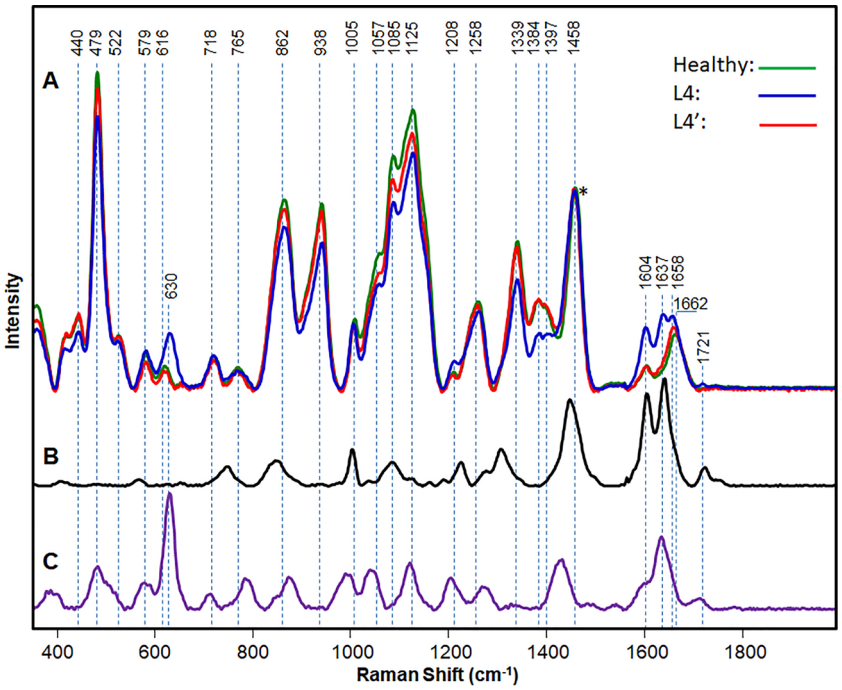

Figure 2. Raman spectra of healthy cowpea, L4 and L4′ (A), normalized to the 1458 cm^{-1} peak (indicated by an asterisk (*)). Raman spectra of bruchid larvae (B) and their excrements (C) are offset for clarity.

Such difference was not detected for the band at 440 cm^{-1} (Table S1). These results suggest that the changes in carbohydrate intensity can be used to detect late larvae and pupae in the infested seeds but not for larvae in their earlier developmental stages. At the same time, the changes between uninfested/early (healthy, L1−L3) and late (L4 and pupa) stages are statistically significant.

We also observed a drastic increase in the intensity of the 1604 cm^{-1} band in the Raman spectra of L4 and pupa, comparing to the Raman spectra of healthy and L1−L3 cowpea seeds. Additionally, we observed significant changes in the amide region (1640−1670 cm^{-1}) in spectra collected from L4 and pupa cowpea seeds. Specifically, a new band at 1637 cm^{-1} appeared, and the 1662 cm^{-1} band shifted to 1658 cm^{-1}. These bands exhibited higher intensities in Raman spectra collected from pupa-seeds than the spectra of L4 seeds. An amide I profile with maxima around 1640 and 1658 cm^{-1} is typical for proteins with predominantly an α-helical secondary structure.[16] At the same time, amide I at 1662 cm^{-1} is typical for large proteins such as globulins and albumin with a mixture of α-helical, β-sheet, and unordered protein secondary structures.[17,18] We also observed an increase in intensity of the band at 630 cm^{-1}. This band can be assigned to skeletal ring deformation of uric acid,[19] as well as C−S stretching of cysteine in proteins or small sulfur containing molecules.[20] Finally, we observed a peak at 1721 cm^{-1} in the Raman spectra of cowpea seeds with L4 and pupa bruchids, which could be assigned to esters.[21−23]

To determine whether these spectral changes reflect insect-feeding on seeds or originate from the bruchid larvae, we cut open the L4 seeds to remove the larvae and their excrements and collected Raman spectra from the L4 seeds with no larvae present (hereafter L4′), bruchid larvae, and their excrements (Figure 2).

We found that observed spectral changes in the 1600−1725 cm^{-1} spectral region were due to the larvae, as their Raman spectrum exhibits intense bands at 1604, 1637, 1658, and 1721 cm^{-1}. These findings suggest that RS can be used to monitor the growth of intact larvae. We also found that the vibrational band at ∼630 cm^{-1}, which was observed in Raman spectra collected from L4 and pupa, could be assigned to uric acid, the major component of insect excrements. Finally, we observed a decrease in the intensity of nearly all vibrational bands that are associated with carboydrates in the L4′ spectrum. Additional mass spectrometric identification of compounds synthesized in seeds in response to a pathogen is required to fully elucidate those spectral changes. Currently, this work is in progress in our laboratory.

Next, we used partial least-squares discriminant analysis[34] (PLS-DA) to determine whether RS can be used for detection of bruchid inside cowpea seeds. Spectra were imported into MATLAB R2017b following baselining by the portable instrument software and then mean centered. Two models were built using PLS_Toolbox 8.6.2, the first model (early late, EL), using 122 spectra partitioned 80:20 into calibration and validation sets by the Kennard-Stone method, determined whether the seed contained no/early (H, L1−L3) or late (L4 or pupa) stage larvae; the second (healthy-early, HE), 88 spectra partitioned 80:20, separates healthy uninfested seeds from those infested by early stage larvae (L1−L3). These two models were used to generate the loadings spectra (Figures S1 and S2) and misclassification tables (Tables 2 and 3).

Table 2. Accuracy of Validation by PLS-DA with the EL Model

	members	correct	early stage	late stage
early stage	16	93.7%	15	0
late stage	8	100%	1	8
Matthew's correlation coefficient	0.913			

DOI: 10.1021/acs.analchem.8b05555
Anal. Chem. XXXX, XXX, XXX−XXX

Table 3. Accuracy of Validation by PLS-DA with HE Model

	members	correct	healthy	early stage
healthy	7	85%	6	0
early stage	10	100%	1	10
Matthew's correlation coefficient	0.883			

The final EL model, containing 8 latent variables (LVs), was used to generate a misclassification table (Table 2) and a loadings plot (Figure S1). The misclassification tables communicate the true positive rate ("correct") and the Matthew correlation coefficient (MCC), a descriptor of the model's ability as a binary classifier. An MCC close to positive one indicates a better classifier. The first three LVs, plotted in Figure S1, explain 83.32%, 5.62%, and 4.43% of the variation between the two classes, respectively. From the loadings plot, the model identified many of the peaks discussed previously as being important predictors of class membership, including those of lignin and/or protein (LV 2 and LV 3) in the 1600 cm^{-1} region, cysteine and/or uric acid at 630 cm^{-1}, and the carbohydrate region from about 1000−1100 cm^{-1}. Unsurprisingly, these correspond to the insect associated peaks observed in Figure 2.

The final HE model, which contained 9 LVs, was used to generate a second misclassification table (Table 3) and loadings plot (Figure S2). The first three LVs of this model explain 60%, 27%, and 6% of the total variation between the healthy and early stage classes. Interestingly, some important peaks for discriminating between healthy and early stages differ from those for early and late stages. For example, while the 1600 cm^{-1} and 630 cm^{-1} regions are important in the EL model, they do not appear to be as important for HE. This is reasonable, as those peaks are closely associated with the bruchid itself. The carbohydrate associated peaks in the 1000−1100 cm^{-1} region retained their importance for both models. Together, these models can discriminate between healthy/uninfested seeds and seeds at early or late stages of infestations with high accuracy.

Our results clearly demonstrate that RS can detect insect pests within plant hosts, such as cowpeas. We showed that observed spectral changes originate from larvae and their excrement. We demonstrated that the combination of chemometric analysis and RS enables us to distinguish between uninfested and infested seeds with high accuracy. Such detection approach is confirmatory, noninvasive, nondestructive and can be performed with a hand-held Raman spectrometer, which makes it a highly desirable pest monitoring tool during storage and transportation of agricultural products. This is extremely important to prevent widespread pest propagation and reduce crop damage by herbivores.

■ ASSOCIATED CONTENT

Supporting Information

The Supporting Information is available free of charge on the ACS Publications website at DOI: 10.1021/acs.analchem.8b05555.

Detailed description of spectra acquisition methods and instrumentation (PDF)

■ AUTHOR INFORMATION

Corresponding Author

*E-mail: dkurouski@tamu.edu. Phone: 979-458-3778.

ORCID

Dmitry Kurouski: 0000-0002-6040-4213

Author Contributions

‖L.S. and C.F. have contributed equally to this work.

Notes

The authors declare no competing financial interest.

■ ACKNOWLEDGMENTS

We are grateful to AgriLife Research of Texas A&M for the provided financial support. We also acknowledge the Governor's University Research Initiative (GURI) grant program of Texas A&M University, GURI Grant Agreement No. 12-2016, M1700437.

■ REFERENCES

(1) Food and Agriculture Organization of the United Nations. *How to Feed the World 2050*; 2009.

(2) Savary, S.; Ficke, A.; Aubertot, J.-N.; Hollier, C. *Food. Secur.* **2012**, *4*, 519−537.

(3) Almeida, M. R.; Alves, R. S.; Nascimbem, L. B.; Stephani, R.; Poppi, R. J.; de Oliveira, L. F. *Anal. Bioanal. Chem.* **2010**, *397*, 2693−2701.

(4) Zeng, Z. C.; Hu, S.; Huang, S. C.; Zhang, Y. J.; Zhao, W. X.; Li, J. F.; Jiang, C.; Ren, B. *Anal. Chem.* **2016**, *88*, 9381−9385.

(5) Virkler, K.; Lednev, I. K. *Anal. Chem.* **2009**, *81*, 7773−7777.

(6) López-López, M.; Delgado, J. J.; García-Ruiz, C. *Forensic Sci. Int.* **2013**, *231*, 1−5.

(7) Cantarero, A. *Procedia Mater. Sci.* **2015**, *9*, 113−122.

(8) Kurouski, D.; Washington, J.; Ozbil, M.; Prabhakar, R.; Shekhtman, A.; Lednev, I. K. *PLoS One* **2012**, *7*, No. e36989.

(9) Bueno, J.; Lednev, I. K. *Anal. Methods* **2013**, *5*, 6292−6296.

(10) Kurouski, D.; Van Duyne, R. P. *Anal. Chem.* **2015**, *87*, 2901−2906.

(11) Farber, C.; Kurouski, D. *Anal. Chem.* **2018**, *90*, 3009−3012.

(12) Egging, V.; Nguyen, J.; Kurouski, D. *Anal. Chem.* **2018**, *90*, 8616−8621.

(13) Thakur, R. P.; Reddy, B. V. S.; Indira, S.; Rao, V. P.; Navi, S. S.; Yang, X. B.; Ramesh, S. *Sorghum Grain Mold Information Bulletin No. 72*; International Crops Research Institute for the Semi-Arid Tropics: Patancheru, India, 2003.

(14) Zhu-Salzman, K.; Murdock, L. L. In *Encyclopedia of Pest Management*; Pimentel, D., Ed.; Taylor & Francis: New York, 2006.

(15) Longe, O. G. *Food Chem.* **1980**, *6*, 153−161.

(16) Berjot, M.; Marx, J.; Alix, A. J. P. *J. Raman Spectrosc.* **1987**, *18*, 289−300.

(17) Kurouski, D.; Van Duyne, R. P.; Lednev, I. K. *Analyst* **2015**, *140*, 4967−4980.

(18) Maiti, N. C.; Apetri, M. M.; Zagorski, M. G.; Carey, P. R.; Anderson, V. E. *J. Am. Chem. Soc.* **2004**, *126*, 2399−2408.

(19) Westley, C.; Xu, Y.; Thilaganathan, B.; Carnell, A. J.; Turner, N. J.; Goodacre, R. *Anal. Chem.* **2017**, *89*, 2472−2477.

(20) Adar, F. *Spectroscopy* **2015**, *30*, 14−19.

(21) Machado, N. F. L.; Calheiros, R.; Gaspar, A.; Garrido, J.; Borges, F.; Marques, M. P. M. *J. Raman Spectrosc.* **2009**, *40*, 80−85.

(22) Butchert, E.; Manley, T. R. *Spectrochim. Acta* **1978**, *34*, 781−784.

(23) Miranda, A. M.; Castilho-Almeida, E. W.; Martins Ferreira, E. H.; Moreira, G. F.; Achete, C. A.; Armond, R. A. S. Z.; Dos Santos, H. F.; Jorio, A. *Fuel* **2014**, *115*, 118−125.

(24) Kizil, R.; Irudayaraj, J.; Seetharaman, K. *J. Agric. Food Chem.* **2002**, *50*, 3912−3918.

(25) Devitt, G.; Howard, K.; Mudher, A.; Mahajan, S. *ACS Chem. Neurosci.* **2018**, *9*, 404−420.

DOI: 10.1021/acs.analchem.8b05555
Anal. Chem. XXXX, XXX, XXX−XXX

(26) Edwards, H. G.; Farwell, D. W.; Webster, D. *Spectrochim. Acta, Part A* **1997**, *53A*, 2383−2392.
(27) Curran, D. J.; Rubin, L.; Towler, M. R. *Clin. Med. Insights: Arthritis Musculoskeletal Disord.* **2015**, *8*, CMAMD.S29061.
(28) De Gussem, K.; Vandenabeele, P.; Verbeken, A.; Moens, L. *Spectrochim. Acta, Part A* **2005**, *61*, 2896−2908.
(29) Zheng, R.; Zheng, X.; Dong, J.; Carey, P. R. *Protein Sci.* **2004**, *13*, 1288−1294.
(30) Cael, J. J.; Koenig, J. L.; Blackwell, J. *Biopolymers* **1975**, *14*, 1885−1903.
(31) Kang, L.; Wang, K.; Li, X.; Zou, B. *J. Phys. Chem. C* **2016**, *120*, 14758−14766.
(32) Agarwal, U. P. *Planta* **2006**, *224*, 1141−1153.
(33) Huang, Y. S.; Karashima, T.; Yamamoto, M.; Ogura, T.; Hamaguchi, H. o. *J. Raman Spectrosc.* **2004**, *35*, 525−526.
(34) Eriksson, L.; Byrne, T.; Johansson, E.; Trygg, J.; Vikstrom, C. *Multi- and Megavariate Data Analysis Basic Principles and Applications*, 3rd revised ed.; Umetrics: Malmö, Sweden, 2013.

DOI: 10.1021/acs.analchem.8b05555
Anal. Chem. XXXX, XXX, XXX−XXX